Long latency of evoked quantal transmitter release from somata of locus coeruleus neurons in rat pontine slices

H.-P. Huang*†, S.-R. Wang*†, W. Yao*†, C. Zhang*†, Y. Zhou*†, X.-W. Chen*†, B. Zhang*†, W. Xiong*†, L.-Y. Wang*†, L.-H. Zheng*†, M. Landry‡, T. Hökfelt§¶, Z.-Q. D. Xu§, and Z. Zhou*†¶‖

*Institute of Neuroscience, Shanghai Institutes for the Biological Sciences, Chinese Academy of Sciences, Shanghai 200031, China; †Institute of Molecular Medicine, Peking University, Beijing 100871, China; ‡Institut National de la Santé et de la Recherche Médicale E358, Institut Francois Magendie, Universite Victor Segalen Bordeaux 2, 33077 Bordeaux, France; §Department of Neuroscience, Karolinska Institutet, S-171 71 Stockholm, Sweden; and ‖State Key Laboratory of Biomembrane Engineering, College of Life Sciences, Peking University, Beijing 100871, China

Contributed by T. Hökfelt, December 4, 2006 (sent for review July 9, 2006)

The locus coeruleus (LC) harbors a compact group of noradrenergic cell bodies projecting to virtually all parts of the central nervous system. By using combined measurements of amperometry and patch-clamp, quantal vesicle release of noradrenaline (NA) was detected as amperometric spikes, after depolarization of the LC neurons. After a pulse depolarization, the average latency of amperometric spikes was 1,870 ms, whereas the latency of glutamate-mediated excitatory postsynaptic currents was 1.6 ms. A substantial fraction of the depolarization-induced amperometric spikes originated from the somata. In contrast to glutamate-mediated excitatory postsynaptic currents, NA secretion was strongly modulated by the action potential frequency (0.5–50 Hz). Somatodendritic NA release from LC upon enhanced cell activity produced autoinhibition of firing and of NA release. We conclude that, in contrast to classic synaptic transmission, quantal NA release from LC somata is characterized by a number of distinct properties, including long latency and high sensitivity to action potential frequency.

amperometry | patch-clamp | somatic release | brain slice | catecholamine

The locus coeruleus (LC) is a well delineated cluster of neuronal somata near the IVth ventricle in the pontine brainstem and consists almost exclusively of noradrenergic cell bodies (the A6 cell group) (1), innervating virtually all parts of the central nervous system (CNS) (2–4). This system plays an important role in the modulation of numerous functions, including the sleep–wake cycle (5, 6), attention (7), learning and memory (8), vigilance (9), mood (10–12), and opioid withdrawal (13–15). Noradrenaline (NA) is released from varicose nerve terminals upon arrival of action potentials generated in the cell soma, as shown with microdialysis techniques (16–19) and amperometry (20). Although much less studied, it is now well established in several systems that neurotransmitters also can be released from soma and dendrites (21). For example, using microdialysis, NA release has been monitored from LC (22, 23). However, the origin of this NA has not be unequivocally established.

Recently, electrochemical measurements using amperometry have been used to detect quantal monoamine release from several cultured cell types by monitoring individual amperometric spikes (ASs) (24–27). Furthermore, the timing of excitation–secretion coupling can be investigated by combined patch-clamp and amperometry (24, 28–30). Depending on the cell type, the latency of monoamine release after action potential stimuli ranges from <2 ms to >50 ms (24, 30), whereas glutamate synaptic transmission is always <2 ms (28, 29). The latency of monoamine release after an action potential has, however, not been studied in the CNS. In single chromaffin cells, the release of monoamines is modulated by the frequency of action potentials (30, 31). It is not clear whether NA release can be modulated by action potential frequency in LC neurons, which fire spontaneously at 0.5–5 Hz and generate evoked action potentials at up to 50 Hz.

In the present work, we performed a combined amperometry and patch-clamp study of somatic transmitter secretion from neurons in LC brain slices to address these questions. We found that the kinetics of stimulus–secretion coupling is very different in CNS somata vs. synapses.

Results

Quantal ASs Evoked from LC Neurons. LC neurons were readily identified by their distinct morphology and electrical properties (see below). To determine whether catecholamine (CA) release from LC neurons occurs via vesicular exocytosis, we made electrochemical recordings through a 5-μm-diameter carbon fiber electrode (CFE) on the somata of LC neurons (Fig. 1). Local application of 80 mM KCl via a puffer pipette (Fig. 1*A*) resulted in a barrage of ASs that coincided with the onset of the puff and then continued for 5–10 s after puffer termination. These ASs, ranging from 0.1 to 5 pA in amplitude, were seen at +780 mV, a potential sufficient to oxidize CAs, but not at 0 mV, a potential at which CA cannot be oxidized (Fig. 1*A*). Thus, CA was released from LC neurons via exocytosis. L-glutamate (10 mM), an endogenous excitatory ligand, also evoked ASs [supporting information (SI) Fig. 6]. The statistic analysis of ASs evoked by 80 mM KCl and 1 mM glutamate showed that these secretogogues significantly increased quantal CA secretion (Fig. 1*A* and SI Fig. 6).

CA Release from Soma. The stimulus-induced ASs detected by CFE sensors here could originate by release either directly from the soma or from invisible terminals or dendrites (32–34) under the CFE sensor tip. To determine the origin of secreted CAs, the soma of acutely isolated LC neurons was patch-clamped, and Ca^{2+} current and a barrage of ASs detected by the CFE on the soma were induced by a depolarization pulse (Fig. 1*B*). According to diffusion theory, the fast ASs must come from release sites within <1 μm of the sensor tip (35, 36), and no nerve processes

Author contributions: H.-P.H., S.-R.W., and W.Y. contributed equally to this work; L.-Y.W., T.H., Z.-Q.D.X., and Z.Z. designed research; H.-P.H., S.-R.W., W.Y., C.Z., Y.Z., X.-W.C., B.Z., W.X., L.-H.Z., and M.L. performed research; Z.Z. contributed new reagents/analytic tools; H.-P.H., S.-R.W., W.Y., L.-Y.W., M.L., T.H., Z.-Q.D.X., and Z.Z. analyzed data; and T.H., Z.-Q.D.X., and Z.Z. wrote the paper.

The authors declare no conflict of interest.

Abbreviations: AS, amperometric spike; CA, catecholamine; CFE, carbon fiber electrode; EPSC, excitatory postsynaptic current; LC, locus coeruleus; LDCV, large dense core vesicles; NA, noradrenaline; TTX, tetrodotoxin.

¶To whom correspondence may be addressed. E-mail: tomas.hokfelt@neuro.ki.se or zzhou@pku.edu.cn.

This article contains supporting information online at www.pnas.org/cgi/content/full/0608897104/DC1.

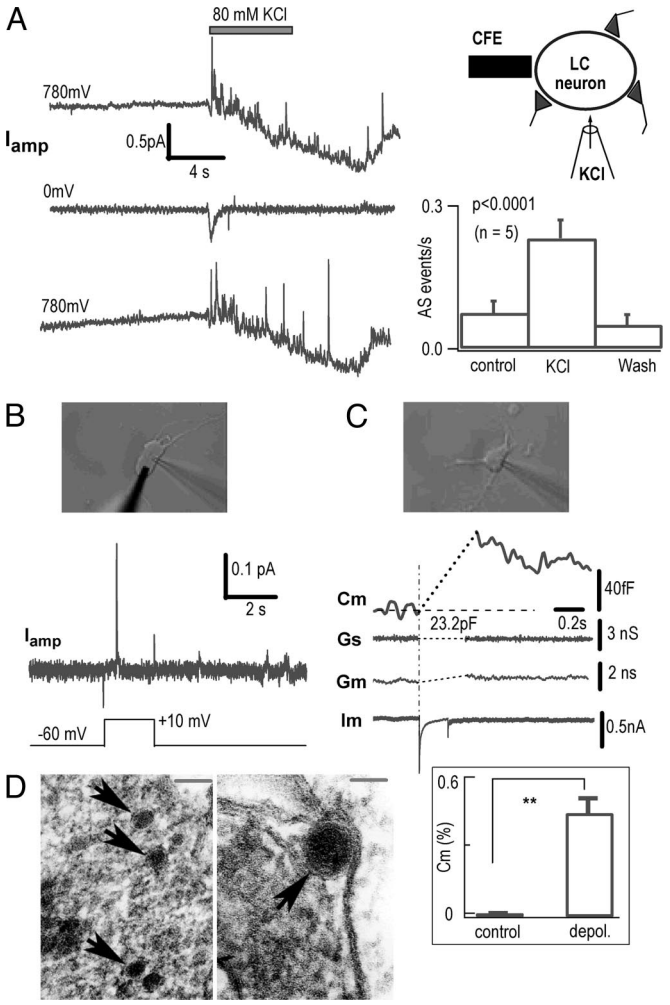

Fig. 1. Amperometric detection of quantal release from soma of LC neurons in brain slice. (*A*) ASs recorded in response to brief 80 mM KCl puffs. KCl-induced ASs occurred reversibly at the CFE holding potential of +780 mV, a potential that oxidizes CA, but not at 0 mV. (*Upper Right*) Experimental protocol. The sensor tip (5-μm diameter) of the CFE was in contact with the soma. The puffer pipette was 150 μm from the soma. (*Lower Right*) KCl (80 mM) significantly increased the rate of quantal release from 0.075 $\pm$ 0.025 ASs/s to 0.232 $\pm$ 0.038 ASs/s ($n = 5$, $P < 0.0001$). The slow changes in response to stimulation are puffer-induced artifacts (27). (*B*) Depolarization induced quantal secretion from the somata of a freshly isolated LC neuron. The CFE signals were recorded from the neuron soma under voltage-clamp mode (*Upper*). Similar result was obtained from three cells. (*C*) Depolarization-induced secretion in somata of freshly isolated LC neurons measured by membrane capacitance. In addition to the capacitance signal (C_m) are membrane conductance (G_m), series conductance (G_s), and membrane current (I_m). The cell was depolarized from -70 to 0 mV for 0.5 s; Cm significantly increased by 0.47 $\pm$ 0.14% of total cell Cm ($n = 12$, $P < 0.01$). (*D*) Electron micrographs of LC neurons. Arrows indicate LDCV, the one to the right closely associated with the membrane. (Scale bars: *D Left*, 140 nm; *D Right*, 75 nm.)

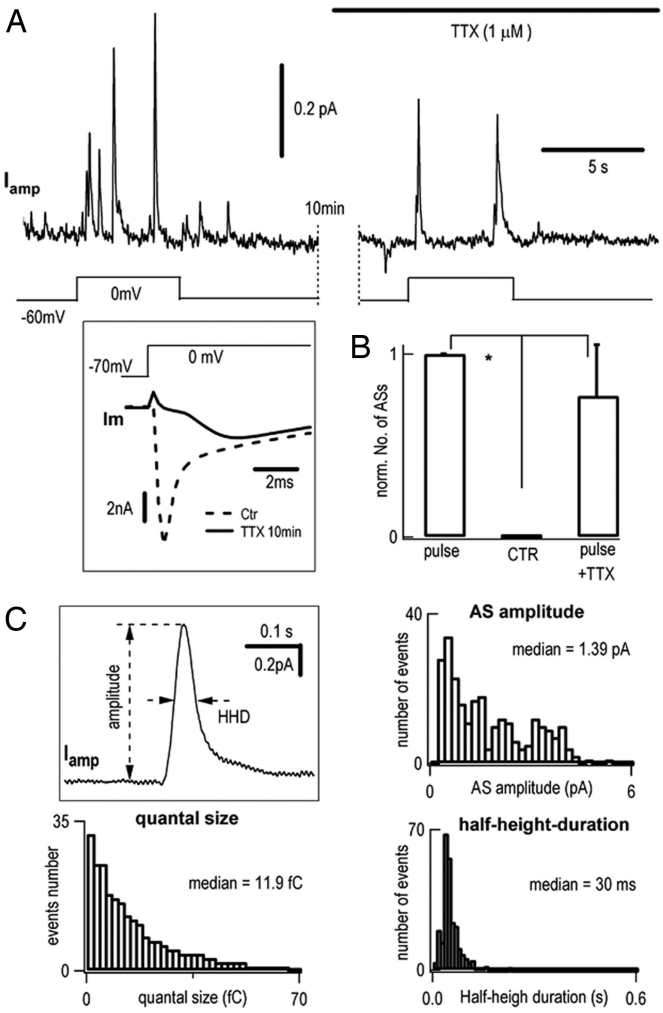

Fig. 2. Fractional contribution of CA release from soma, and kinetics of the quanta. (*A*) TTX (0.1–1 μM) could not block the depolarization pulse-induced secretion detected by a CFE on the soma, whereas Na^+ currents were fully blocked (*Inset*). (*B*) Statistics of experiments illustrated in *A*. TTX blocked 23 $\pm$ 28% of total secretion induced by depolarization of the soma under whole-cell voltage-clamp (*, $P < 0.05$; $n = 4$). CTR, control. (*C*) Kinetic parameters of individual ASs. (*Upper Left*) Typical AS event with definition of parameters. The median amplitude and quantal charge were 1.39 pA and 11.9 fC, respectively. The median half-height duration was 30 ms. Considering the that signal was prefiltered (10-Hz bandwidth), the actual ASs are slightly faster (27).

were visible at the CFE site. Thus, the ASs must have originated from somatic release. Another assay for neural somatic secretion is membrane capacitance measurement, which detects vesicle fusion on the voltage-clamped soma (37, 38). Indeed, depolarization induced significant capacitance increase, indicating exocytosis at the soma of the isolated LC neuron (Fig. 1*C*). The ultrastructural analysis revealed the presence of large dense core vesicles (LDCV) ($\approx$100-nm diameter) in the soma and dendrites, upon K^+-stimulation sometimes close to the membrane (Fig. 1*D*) (32, 33). We conclude that a substantial fraction of the depolarization-induced CA release is from the neuron somata in LC slices.

Furthermore, to determine whether the soma could secrete CAs, 1 μM tetrodotoxin (TTX) was added to the perfusion solution to block all dendritic ASs in response to soma depolarization by the voltage-clamp (Fig. 2 *A* and *B*). Although TTX fully blocked the voltage-gated Na^+ current, the total number of ASs induced by soma depolarization was reduced only by 23 $\pm$ 28% (Fig. 2 *A* and *B*). The quantal average size was 2.0 $\pm$ 0.5 times larger in presence of TTX ($n = 5$, $P < 0.05$), indicating that quantal size is larger in somata vs. nonsomata (terminals, dendrites), consistent with previous findings in a nonvertebrate neuron (39). This finding implies that the TTX-resistant ASs may reflect release directly from the soma.

The kinetics of single AS events, representing single-vesicle release (Fig. 2*C*), showed a median quantal size of 11.9 fC, corresponding to 3.7×10^4 CA molecules (see *Materials and Methods*). After low-pass filtering with a corner frequency of 10 Hz

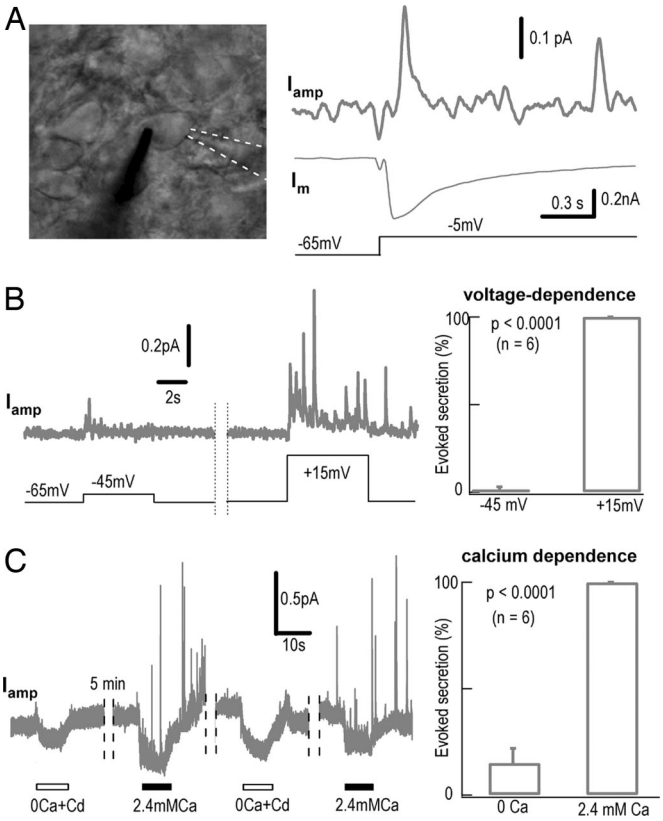

Fig. 3. Ca^{2+} dependence of stimulus-induced quantal CA release. (*A*) Simultaneous amperometric and patch-clamp recordings in a neuron in the LC brain slice. Depolarization from −65 to −5 mV induced a whole-cell Ca^{2+} current (I_m; middle trace) and ASs (I_{amp}; upper trace). The left image illustrates a neuron recorded by a CFE (lower, dark) and a patch-pipette (right, dashed lines). (*B*) Voltage dependence of depolarization-induced secretion. (*Left*) Amperometric recording (upper traces) and stimulation protocol (lower traces). (*Right*) Statistics of voltage dependence ($n = 6$, $P < 0.0001$). (*C*) Secretion depended on extracellular Ca^{2+}. A barrage of ASs was reversibly induced by application of bath solution containing 80 mM KCl and 2.4 mM Ca^{2+} but not by application of bath solution containing 80 mM KCl, 0 Ca^{2+}, 1 mM EGTA, and 200 μM $CdCl_2$. (*Right*) Statistics of this experiment ($n = 6$, $P < 0.0001$).

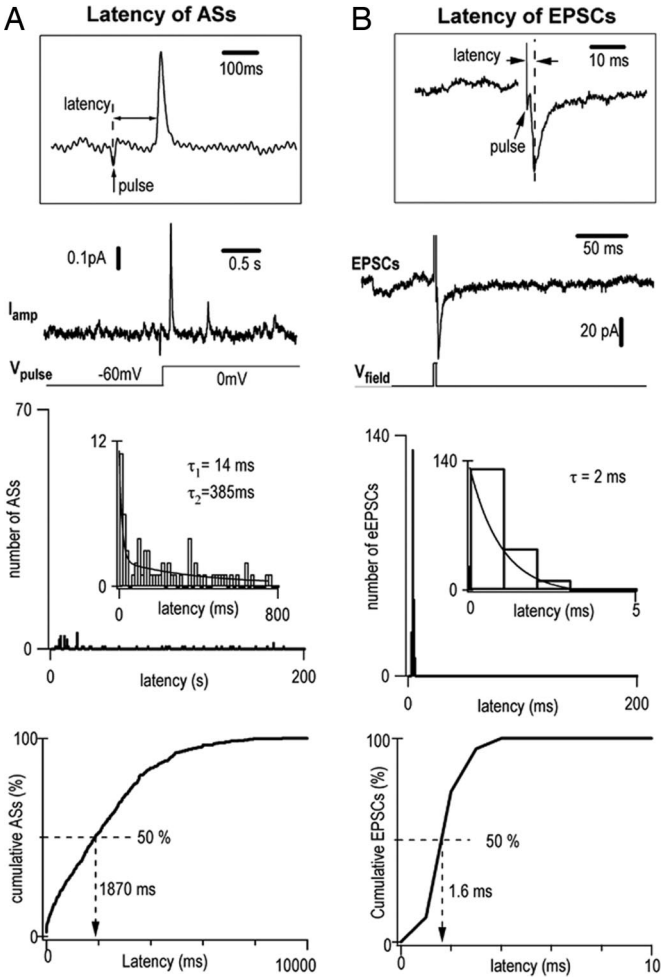

Fig. 4. Latency of depolarization-induced release of CA vs. glutamate in LC neurons. (*A*) Latency of quantal release of CA, measured by amperometry (I_{amp}) in response to depolarization pulses (V_{pulse}). V_{pulse} from −60 to 0 mV induced ASs. The latency between the onset of depolarization and the first AS is expanded in *Top Inset*. (*Middle*) Histograms of the latency to the first ASs. The two time constants of the histogram latency were 14 (83%) and 385 (17%) ms, respectively (452 events). (*Bottom*) Cumulative distribution from above latency histogram. The ''50% latency'' was 1,870 ms, corresponding to presynaptic CA release from LC soma. (*B*) Latency of EPSCs of glutamate, measured by postsynaptic currents in response to field stimulation pulses (V_{field}). The latency between the onset of field stimulation and the EPSC is expanded in *Top Inset*. (*Middle*) Histograms of the latency of evoked EPSCs. The time constant of the latency histogram was 2 ms (192 events). (*Bottom*) Cumulative distribution from above latency histogram. The ''50% latency'' was 1.6 ms, corresponding to postsynaptic glutamate currents in LC soma.

for suppressing the background noise, AS amplitude ranged between 0.1 and 5 pA. The median of half-width duration was 30 ms.

Ca^{2+} Dependence of Evoked ASs. We investigated the Ca^{2+} dependence of quantal CA release from LC soma by combining patch-clamp and amperometric recordings in LC neurons (Fig. 3). At the soma of an LC neuron (Fig. 3*A*, DIC photograph), ASs occurred during the Ca^{2+} influx induced by a depolarizing pulse (Fig. 3*A*). Paralleling the voltage-dependent activation of Ca^{2+} current, significantly more ASs were induced for steps to +15 mV than to −45 mV (holding potential −65 mV for both experiments). The number of ASs at −45 mV was 1.5 ± 1.5% of the number at +15 mV (Fig. 3*B*).

Further evidence that the depolarization-evoked ASs depended on Ca^{2+} influx through Ca^{2+} channels is shown in Fig. 3*C*. First, a neuron without patch-clamp was puffed with a high (80 mM) KCl solution containing 0 Ca^{2+} and 200 μM Cd^{2+} (a Ca^{2+} channel blocker; see ref. 40), and few ASs were evoked. Subsequently, another 80 mM KCl solution containing 2 mM Ca^{2+} and 0 Cd^{2+} was applied to the same neuron, and a barrage of ASs was evoked. These experiments were repeated twice in the same neuron. The numbers of ASs induced by 80 mM KCl were 1.33 ± 0.69 and 7.67 ± 1.14 in 0 Ca^{2+}/200 μM Cd^{2+} and 2 mM Ca^{2+}/+0 Cd^{2+}, respectively.

Latencies of Evoked CA vs. Glutamate Release. Compared with the fast synaptic transmission, the latency of CA release was diverse in different peripheral tissues (24, 28–30). Here, we compared the latencies of CA vs. glutamate in LC neurons, by monitoring CA release by CFE (as physical sensor) and glutamate release from presynaptic nerve endings by excitatory postsynaptic currents (EPSCs) (as biosensor), after a depolarization pulse. When using minimum stimulation for each of the two types of transmitter release, drastic differences in the latencies of the depolarization-evoked ASs and field-stimulation-induced EPSCs were found in LC neurons (Fig. 4). A depolarization step from −60 to 0 mV evoked quantal ASs with a long latency (>100 ms for most events; Fig. 4*A*). The histograms of the AS latency and its cumulative latency distribution are shown in Fig. 4 *Middle* and *Bottom*. There were two distinct time constants (τ_1 = 14 ms

NEUROSCIENCE

and τ_2 = 385 ms) in the AS latency histogram. In contrast, a single-field stimulation pulse evoked EPSC from another LC neuron under whole-cell recording, with a latency of <2 ms (Fig. 4*B*). The time constant of the EPSC latency was ≈2 ms at room temperature. These EPSCs were blocked by kynurenic acid, an antagonist of glutamate receptor channels (SI Fig. 7). The "50% latencies," at which 50% of all events have a shorter latency, were 1,870 and 1.6 ms, corresponding to presynaptic CA release from LC soma and postsynaptic glutamate currents in LC soma, respectively. Thus, the latency of evoked CA release from LC soma is substantially (10–1,000 times) slower than synaptic glutamate release onto LC neurons.

Modulation of Quantal Release by Frequency of Action Potentials. To investigate whether CA secretion is modulated by patterns of cell activity, we measured ASs in response to different frequencies of action potentials and found that the evoked CA secretion is strongly dependent on the action potential frequency. In voltage-clamp mode, a barrage of ASs was evoked by 100 action potential waveforms at 20 Hz. However, no ASs were evoked by 100 action potentials at 4 Hz. Subsequently, a barrage of ASs was evoked again by 100 action potentials at 20 Hz (Fig. 5*A*). Similar results were observed in current-clamp mode, that is, a barrage of ASs was evoked by high-frequency action potentials (≈50 Hz, induced by injecting 200 pA for 10 s; Fig. 5*B*) but not by the spontaneous action potentials (≈3 Hz; Fig. 5*B*, upper trace). These phasic high-frequency action potentials could also be induced by applying the endogenous transmitter glutamate (SI Fig. 8). The statistics of the frequency dependence of ASs showed that CA secretion is essentially only evoked at high frequency (excited status) (Fig. 5 *C* and *D*). During spontaneous firing (3 Hz), there was little CA secretion. In contrast, as measured by EPSCs in postsynaptic LC neurons, the efficiency of glutamate release triggered by action potentials was similar at 4 and 20 Hz, indicting that soma release of CA is much more sensitive to patterns of action potentials than classic synaptic release (SI Fig. 9).

Physiological Relevance of LC Somatic Secretion. Virtually all large cell bodies (20–50 μm in diameter) in LC expressed tyrosine hydroxylase; that is, were catecholaminergic (see a typical LC neuron loaded with luciferase yellow in SI Fig. 10*A*). In whole-cell recording, NA (30 μM) evoked a 50-pA outward current in voltage-clamp mode and a −20-mV membrane hyperpolarization from a resting potential of around −50 mV, which blocked the spontaneous firing (0.5–5 Hz), in current-clamp mode (SI Fig. 10*A*). These experiments imply that NA release leads to autoinhibition of excitability in LC neurons (41).

To test whether NA-mediated autoinhibition occurs via α2-adrenoceptors (α2ARs), we stimulated the neurons to secrete CAs in the presence or absence of yohimbine, an α2AR antagonist (SI Fig. 10*B*). Depolarization-evoked CA release was significantly and reversibly increased by applying 2 μM yohimbine for 10 min in the LC slices, as detected by amperometry with a cylindrical CFE (SI Fig. 10*C*). In contrast to the "point-sensor" CFE, which had a sensor tip with a disk shape of ≈25 μm^2 and measured quantal CA release at single cell surfaces, the "cylindrical sensor" CFE, which had a sensor tip size of ≈1,000 μm^2, measured average CA release from many cells (42). These experiments suggest that evoked CA release has a negative feedback action through the α2AR autoreceptors in LC neurons.

Discussion

This combined amperometry and patch-clamp study of somatic transmitter secretion from neurons in a brain slice preparation permitted us to determine the timing of CA release in response to action potentials/depolarization in the soma of LC neurons. It is most likely that the oxidizable substance detected as ASs represents released NA, the major CA neurotransmitter synthesized in (1) and released from (43) LC neurons. The quantal size was 11.9 fC (or 37,000 NA molecules) per vesicle, similar to that found in the vesicles in sympathetic varicosities in the iris (71) and in superior cervical ganglion neurons (27, 44) and for dopamine in substantia nigra (45) neurons but much smaller than that of chromaffin cells (24, 26, 30).

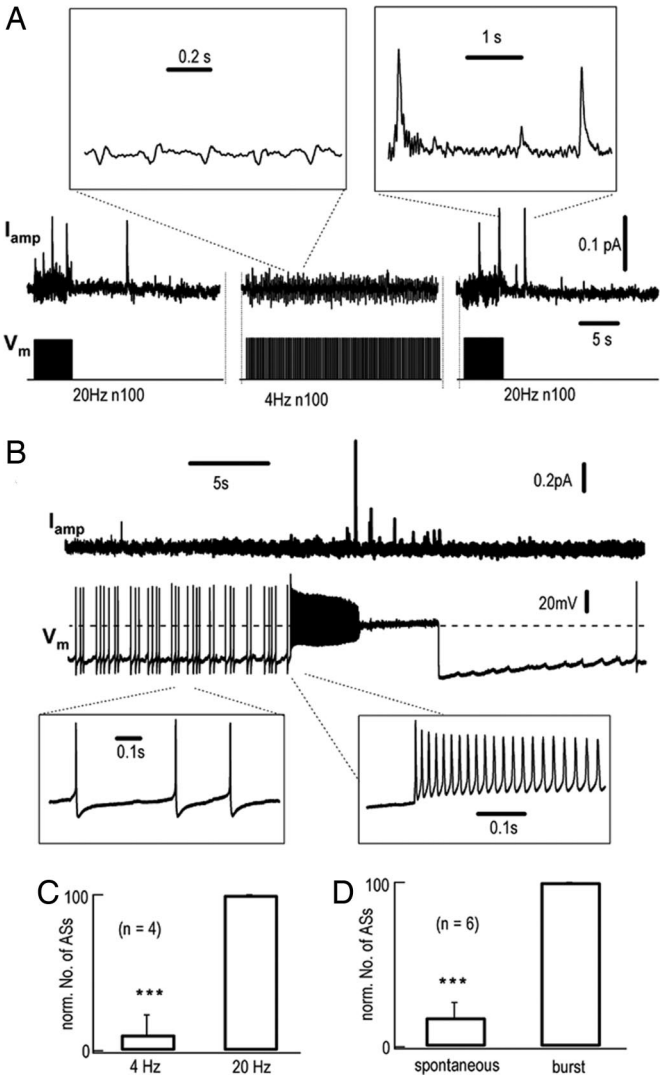

Fig. 5. CA secretion is critically controlled by frequency of action potentials. (*A*) Frequency-dependent secretion in voltage-clamp mode. The stimulation protocol (lower traces) consisted of three trains of 100 brief (10 ms) depolarization pulses from −60 to 0 mV at 20 Hz (*Left* and *Right*) and 4 Hz (*Center*). The interval between trains was 5 min. The *Insets* show the amperometry trace (note the small stimulus artifacts in the background noise during stimulation at 4 Hz). (*B*) Frequency-dependent secretion in current-clamp mode. Few ASs occurred during spontaneous firing at ≈4 Hz. In response to depolarization by injecting a +200-pA current, the frequency of action potentials was increased to 50 Hz (*Inset*), which in turn triggered ASs. (*C* and *D*) Statistics of experiments of *A* ($n = 4$, $P < 0.001$) and *B* ($n = 6$, $P < 0.001$). High action potential frequency significantly increased cell secretion. norm. No. of ASs, ratio of ASs induced by 100 brief pulses under voltage-clamp (*C*) or injecting a 200-pA current under current-clamp (*D*). The interval times between two recordings were 3 min.

Evoked NA Release from Soma of LC Neurons. Here, we provide compelling evidence that NA release can occur directly from the neuronal soma in the LC: (*i*) ASs were detected by the sensor tip on the soma; (*ii*) TTX blocked <20% of total secretion induced

by depolarization of the soma (Fig. 2*A*); (*iii*) in freshly isolated LC neurons, ASs were induced by depolarization of voltage-clamped somata (Fig. 1*B*); (*iv*) in freshly isolated LC neurons, capacitance increases were induced by depolarization of voltage-clamped somata (Fig. 1*C*); and (*v*) vesicles were found in LC neurons, occasionally close to the membrane (Fig. 1*D*). Because TTX blocked 23% of the total NA release (Fig. 2), we estimate that the fractional contribution of NA release is 77% from the soma and 23% from dendrites/terminals in the LC region.

Timing of NA Release in LC Neuron Soma. Activity-evoked neurotransmission consists of a series of synaptic events including presynaptic action potential firing, Ca^{2+} influx, exocytosis, transmitter diffusion, receptor activation, and postsynaptic firing activation (46). For synaptic transmission mediated via an excitatory transmitter such as glutamate, the time required to complete these six steps is typically within 1–2 ms at room temperature (47, 48) (Fig. 4). In early studies on release from adrenal chromaffin cell body, much slower (50 ms) excitation–secretion coupling has been found (24, 30). More recent studies on calf chromaffin cells, however, recorded a mean delay of "strongly coupled" signals of ≈3 ms; that is, the rate of exocytosis approached that of neurons (29). In studies on cultured leech neurons, serotonin release was monitored from both small granular vesicles and LDCV and discharges with time constants of, respectively, ≈260 μs and 1.3 ms were recorded (28). In the present work, on soma of a mammalian CNS neuron, we report that the speed of somatic NA release from LC neurons is much slower than that of glutamate synaptic transmission (1,870 vs. 1.6 ms at room temperature). In addition, using minimum stimulations for triggering ASs and EPSCs, we found that ASs need much stronger stimulation than EPSCs. Because the latency histograms in Fig. 4 were produced with minimum stimulations, we conclude that the >100-times-longer latency of ASs vs. EPSCs is the intrinsic property of the soma secretion rather than a result of stronger stimulation (see also Fig. 5*B*, where the weak stimulation of action potentials caused even longer secretion latency).

In prefrontal cortex, CA synapses colocalize with the fast glutamatergic synapses, and may play a critical role in genesis of long-term potentiation and/or long-term depression *in situ*, as well as drug addiction *in vivo* (49). The longer latency of CA release, which inhibits synaptic transmission, provides an alternative mechanism of the development of long-term potentiation/long-term depression using a "middle-long-lasting" Ca^{2+} transient in the synapse. The fast excitatory glutamate and the delayed inhibitory CA could, respectively, be responsible for the onset and offset of the Ca^{2+} transient.

Sensitivity of NA Release to Action Potential Patterns. A possible reason for the slow release at the somatodendritic region is that Ca^{2+} channels and NA-storing vesicles are not closely localized at this site (29). Moreover, in the cell soma, there is no evidence for synaptic specializations such as the presynaptic grid (50) that controls docking of synaptic vesicles into a release position. The slow neurotransmission is a consequence of the dependence of NA release on the action potential patterns in the somatodendritic region of the LC neurons. If Ca^{2+} channels and vesicles are not closely localized, the $[Ca^{2+}]_i$ level required for secretion will only be attained by action potentials with a sufficiently high frequency. Low-frequency action potentials cannot trigger NA release, because local Ca^{2+} drops to basal levels during the interval between two action potentials (31). Indeed, although LC neurons spontaneously fired at low frequency (3–5 Hz), little NA was released (Fig. 5). In contrast, when action potential frequency was increased by an excitatory input, a distinct NA release was recorded (Fig. 5 and SI Fig. 8). This regulation differs from fast synaptic transmission in LC neurons, because synaptic glutamatergic transmission is less dependent on action potential frequency (SI Fig. 9) (51).

Subcellular Localization of NA in LC Neurons. NA in central neurons is stored both in small synaptic (granular) vesicles and LDCV (52), and such vesicles are also present in both the cell soma and dendrites of LC neurons (32, 33, 53). Here, we provide some evidence for exocytotic release from LDCV after K^+ stimulation and tannic acid treatment. However, we do not show that these LDCV store NA because we did not use the KMnO4 fixation technique. Also, we do not know the extent to which the small (granular) NA-storing synaptic vesicles (33) participate in the somatic release process. However, the fact that NA secretion preferentially occurs at high action potential frequency may suggest that LDCV are mainly involved (54).

In earlier microdialysis and amperometric studies (16–20), NA release was monitored from the LC. However, the origin of this NA could not be unequivocally established. Thus, in the LC, there are also nerve endings with small granular vesicles and LDCV (32, 33), which may not only represent recurrent collaterals storing NA (33, 34) but also adrenaline afferents (55) and perhaps even 5-hydroxytryptamine-containing nerve endings.

Functional Significance of Somatic/Dendritic NA Release. A physiological role for NA released from LC soma/dendrites may be to provide negative feedback via the autoreceptors on the LC cell body (56, 57), and voltammetric analysis has demonstrated that this is exerted via α2A adrenoreceptors (58, 59). Our observations that NA hyperpolarized the cell and that blockade of α2AR increased NA release are in agreement with these findings (SI Fig. 10). However, whereas inhibition via an autoreceptor was originally assumed to involve NA release from recurrent collaterals (57), our findings strongly suggest that somatic/dendritic release plays an important role. In fact, NA release at a somatic site represents a transient inhibitory "synapse," resulting in hyperpolarization and reduction of action potential frequency and firing, preventing further NA release, and providing evidence that local regulatory mechanisms are important for LC functionality. The fact that somatic NA release depends on the action potential pattern may have clinical relevance as well, e.g., because the LC somatodendritic region is considered to be a predominant site for cocaine action on the brain (60).

Materials and Methods

Brain Slice Preparation. All experiments were performed by using Sprague–Dawley rats (postnatal days 8–14) according to the guidelines of the Animal Research Advisory Committees of the Shanghai Institutes of Biological Sciences and Peking University and of the local ethical committee in Stockholm. Three-hundred-micrometer-thick slices were prepared and processed as described (61). The preparation of freshly isolated LC neurons was performed as described (41).

Electrophysiological Recordings. LC neurons were readily identified by their anatomical position as well as their distinctive electrical discharge pattern and membrane properties (62). Whole-cell recordings were performed by using an EPC9/2 amplifier and Pulse software (HEKA Elektronik, Lambrecht/Pfalz, Germany). Cells were voltage-clamped at −60 mV by using patch pipettes of 2–4 MΩ (the corrected holding potential was −60 mV, after junction potential correction according to ref. 63). Data were analyzed with IGOR software (WaveMetrics, Lake Oswego, OR). The pipette internal solution contained 135 mM CsCl, 1 mM $MgCl_2$, and 10 mM Hepes (pH 7.2). All chemicals were from Sigma (St. Louis, MO). A microperfusion device (MPS-2; INBIO, Wuhan, China) with a fast exchange time (<100 ms) among eight channels was used to puff drugs locally to the cell under study (64).

Amperometry and Capacitance Recordings. Basic amperometric recordings were performed as described (30, 65). The sensor tip of a 5-μm polypropylene-insulated CFE (Dagan, Minneapolis, MN) (66) was held at 780 mV, and the tip gently touched the soma. These standard point-type CFEs had a 10- to 20-μm exposed tip. In some experiments, cylinder-type CFEs with a long sensor tip (200 μm) were used to detect local CA release from many cells (42). Amperometric currents were low-pass-filtered at 100 Hz and sampled by the EPC-9/2 at 4 kHz. To reduce noise, these data were further digitally filtered at 10 Hz for analysis. For analysis of the kinetic properties of ASs, only events >2 SD were included (67). The amount of the CA was estimated to be equivalent to two electrons per oxidized molecule (24, 27, 30).

In some cases, we measured membrane capacitance (C_m) in isolated cells using the software lock-in module of Pulse 8.30 together with an EPC9/2 amplifier as described (68).

Field Stimulation. Bipolar stimulating electrodes were made from Teflon-coated platinum wire (50-μm diameter) with a tip separation of $\approx$50 μm. The stimulating electrode was placed on the slice surface. The cylinder CFE was positioned between the electrical poles and inserted 50–100 μm into the slice (42). A pulse-train (200 pulses at 100 Hz) was used to evoke neurotransmitter release. The pulse duration was 500 μs, and the amplitude was 15 μA to 1 mA.

Electron Microscopic Analysis. Horizontal Vibratome (St. Louis, MO) slices were made and incubated in KRB buffer for 60 min at 37°C under an atmosphere of 5% CO_2/95% O_2, followed by high K^+ (56 mM) buffer plus tannic acid (1.2 mM) (69, 70), and fixed with 5% formalin plus 2% glutaraldehyde (71), followed by osmium tetroxide. After block-staining with uranyl acetate, dehydration, and embedding, sections were cut, counterstained with lead citrate, and examined in a T-600 electron microscope.

See *SI Methods* for further details.

We thank Drs. Reinhard Jahn, Bob Chow, and Iain Bruce for comments on the manuscript. This work was supported by National Basic Research Program of China Grant 2006CB500800; National Natural Science Foundation of China Grants 30330210 (to Z.Z.), 30470445 (to Z.Z.), and 30328013 (to L.-Y.W.; visiting professor from the University of Toronto); Swedish Research Council Grant 04X-2887; European Community NEWMOOD Grant LHSM-CT-2003-503474; Swedish Foundation for International Cooperation in Research and Higher Education Grant IG2004-2070; the Marinne and Marcus Wallenberg Foundation; Hjärnfonden; Svenska Läkaresällskapet; and Swedish Research Links Programme 348-2006-6688.

1. Dahlström A, Fuxe K (1964) *Acta Physiol Scand* 232:1–55.
2. Moore JP, Card RY (1984) in *Classical Transmitters in the CNS*, Handbook of Chemical Neuroanatomy, eds Bjorklund A, Hökfelt T (Elsevier, Amsterdam), Vol 2, pp 123–156.
3. Morrison JH, Molliver ME, Grzanna R (1979) *Science* 205:313–316.
4. Ungerstedt U (1971) *Acta Physiol Scand Suppl* 367:1–48.
5. Jouvet M (1969) *Science* 163:32–41.
6. Hobson JA (1975) *Arch Gen Psychiatry* 32:1421–1424.
7. Carli M, Robbins TW, Evenden JL, Everitt BJ (1983) *Behav Brain Res* 9:361–380.
8. Sara SJ, Devauges V (1989) *Behav Neural Biol* 51:401–411.
9. Aston-Jones G, Foote SL, Segal M (1985) *Neuroscience* 15:765–777.
10. Foote SL, Bloom FE, Aston-Jones G (1983) *Physiol Rev* 63:844–914.
11. Saper CB, Petito CK (1982) *Brain* 105:87–101.
12. Mongeau R, Weiss M, de Montigny C, Blier P (1998) *Neuropharmacology* 37:905–918.
13. Maldonado R, Koob GF (1993) *Brain Res* 605:128–138.
14. Stanford SC (1995) *Pharmacol Ther* 68:297–242.
15. Willis WD, Westlund KN (1997) *J Clin Neurophysiol* 14:2–31.
16. Berridge CW, Abercrombie ED (1999) *Neuroscience* 93:1263–1270.
17. Abercrombie ED, Keller RW, Jr, Zigmond MJ (1988) *Neuroscience* **27,** 897–904.
18. L'Heureux R, Dennis T, Curet O, Scatton B (1986) *J Neurochem* 46:1794–1801.
19. van Veldhuizen MJ, Feenstra MG, Boer GJ, Westerink BH (1990) *Neurosci Lett* 119:233–236.
20. Brun P, Suaud-Chagny MF, Gonon F, Buda M (1993) *Neuroscience* 52:961–972.
21. Ludwig M (2005) *Dendritic Transmitter Release* (Springer, New York).
22. Pudovkina OL, Kawahara Y, de Vries J, Westerink BH (2001) *Brain Res* 906:38–45.
23. Van Gaalen M, Kawahara H, Kawahara Y, Westerink BH (1997) *Brain Res* 763:56–62.
24. Chow RH, von Ruden L, Neher E (1992) *Nature* 356:60–63.
25. Pothos EN, Davila V, Sulzer D (1998) *J Neurosci* 18:4106–4118.
26. Wightman RM, Jankowski JA, Kennedy RT, Kawagoe KT, Schroeder TJ, Leszczyszyn DJ, Near JA, Diliberto EJ, Jr, Viveros OH (1991) *Proc Natl Acad Sci USA* 88:10754–10758.
27. Zhou Z, Misler S (1995) *Proc Natl Acad Sci USA* 92:6938–6942.
28. Bruns D, Jahn R (1995) *Nature* 377:62–65.
29. Elhamdani A, Zhou Z, Artalejo CR (1998) *J Neurosci* 18:6230–6240.
30. Zhou Z, Misler S (1995) *J Biol Chem* 270:3498–3505.
31. Duan K, Yu X, Zhang C, Zhou Z (2003) *J Neurosci* 23:11235–11243.
32. Hökfelt T (1967) *Z Zellforsch Mikrosk Anat* 79:110–117.
33. Shimizu N, Katoh Y, Hida T, Satoh K (1979) *Exp Brain Res* 37:139–148.
34. Swanson LW (1976) *Brain Res* 110:39–56.
35. Chow RH, von Ruden L (1995) in *Single Channel Recording*, eds Sakmann B, Neher E (Plenum, New York), pp 245–275.
36. Schroeder TJ, Jankowski A, Kawagoe KT, Wightman RM, Lefrou C, Amatore C (1992) *Anal Chem* 64:3077–3083.
37. Lindau M, Neher E (1988) *Pflügers Arch* 411:137–146.
38. Zhang C, Zhou Z (2002) *Nat Neurosci* 5:425–430.
39. Bruns D, Riedel D, Klingauf J, Jahn R (2000) *Neuron* 28:205–220.
40. Chow RH (1991) *J Gen Physiol* 98:751–770.
41. Arima J, Kubo C, Ishibashi H, Akaike N (1998) *J Physiol* 508:57–66.
42. Palij P, Stamford JA (1994) *Brain Res* 634:275–282.
43. Singewald N, Philippu A (1998) *Prog Neurobiol* 56:237–267.
44. Koh DS, Hille B (1997) *Proc Natl Acad Sci USA* 94:1506–1511.
45. Jaffe EH, Marty A, Schulte A, Chow RH (1998) *J Neurosci* 18:3548–3553.
46. Südhof TC (2004) *Annu Rev Neurosci* 27:509–547.
47. Augustine GJ, Charlton MP (1986) *J Physiol* 381:619–640.
48. Sabatini BL, Regehr WG (1996) *Nature* 384:170–172.
49. Dong Y, Nasif FJ, Tsui JJ, Ju WY, Cooper DC, Hu XT, Malenka RC, White FJ (2005) *J Neurosci* 25:936–940.
50. Pfenninger K, Sandri C, Akert K, Eugster CH (1969) *Brain Res* 12:10–18.
51. Wang LY, Kaczmarek LK (1998) *Nature* 394:384–388.
52. Hökfelt T (1968) *Z Zellforsch Mikrosk Anat* 91:1–74.
53. Groves PM, Wilson CJ (1980) *J Comp Neurol* 193:853–862.
54. Lundberg JM, Hökfelt T (1983) *Trends Neurosci* 6:325–333.
55. Hökfelt T, Fuxe K, Goldstein M, Johansson O (1974) *Eur J Pharmacol* 25:108–112.
56. Svensson TH, Bunney BS, Aghajanian GK (1975) *Brain Res* 92:291–306.
57. Cedarbaum JM, Aghajanian GK (1977) *Eur J Pharmacol* 44:375–385.
58. Callado LF, Stamford JA (1999) *Eur J Pharmacol* 366:35–39.
59. Callado LF, Stamford JA (2000) *J Neurochem* 74:2350–2358.
60. Thomas DN, Post RM, Pert A (1994) *Brain Res* 645:135–142.
61. Xu ZQ, Pieribone VA, Zhang X, Grillner S, Hökfelt T (1994) *Exp Brain Res* 98:75–83.
62. Williams JT, North RA, Shefner SA, Nishi S, Egan TM (1984) *Neuroscience* 13:137–156.
63. Neher E (1995) in *Single Channel Recording*, eds Sakmann B, Neher E (Plenum, New York), pp 147–153.
64. Wu B, Wang YM, Xiong W, Zheng LH, Fu CL, Bruce IC, Zhang C, Zhou Z (2005) *Front Biosci* 10:761–767.
65. Chen J, Yan F, Dai Z, Ju H (2005) *Biosens Bioelectron* 21:330–336.
66. Zhou Z, Misler S (1996) *J Biol Chem* 271:270–277.
67. Zhou Z, Misler S, Chow RH (1996) *Biophys J* 70:1543–1552.
68. Gillis KD (1995) in *Single Channel Recording*, eds Sakmann B, Neher E (Plenum, New York), pp 155–198.
69. Buma P, Nieuwenhuys R (1987) *Neurosci Lett* 74:151–157.
70. Pow DV, Morris JF (1989) *Neuroscience* 32:435–439.
71. Hökfelt T, Ljungdahl Å (1972) *Adv Biochem Psychopharmacol* 6:1–34.